Buletin Ilmiah Sarjana Teknik Elektro
Vol. 8, No. 1, February 2026, pp. 294-310
ISSN: 2685-9572, DOI: 10.12928/biste.v8i1.15529

Genetic Algorithm Tuned Controllers for High-Performance Indirect Field-Oriented Control in DFIG-Based WECS

Samira Heroual [1], **Belkacem Belabbas** [1], **Kheloud Ayati** [1], **Rabia Haloui** [1], **Ahmed Tawfik Hassan** [2], **Alfian Ma'arif** [3], **Mohamed Metwally Mahmoud** [4,5,6], **Vojtech Blazek** [6]

[1] Department of Electrical Engineering, L2GEGI laboratory, University of Tiaret, Tiaret, Algeria;
[2] Department of Electrical Engineering, Faculty of Engineering, Aswan University, Aswan 81542, Egypt
[3] Department of Electrical Engineering, Universitas Ahmad Dahlan, Yogyakarta, Indonesia
[4] Department of Electrical Engineering, Faculty of Energy Engineering, Aswan University, Aswan 81528, Egypt
[5] Jadara University Research Center, Jadara University, P.O Box 733, Irbid, Jordan
[6] ENET Centre, CEET, VSB—Technical University of Ostrava, Ostrava, 708 00, Czech Republic

ARTICLE INFORMATION

Article History:

Received 04 December 2025
Revised 26 February 2026
Accepted 05 March 2026

Keywords:

Wind Turbine;
Doubly-Fed Induction Generator;
Indirect Field-Oriented Power Control;
Classical Proportional-Integral;
Genetic Algorithm

Corresponding Author:

Mohamed Metwally Mahmoud,
Department of Electrical Engineering, Faculty of Energy Engineering, Aswan University, Aswan 81528, Egypt.
Email: metwally_m@aswu.edu.eg

ABSTRACT

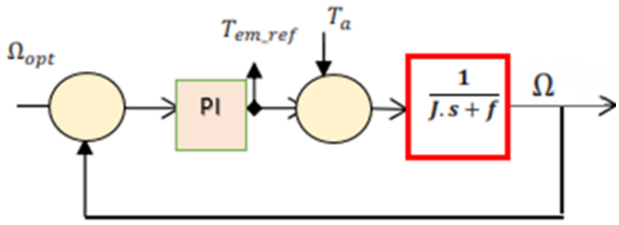

Due to rising environmental awareness, rising fuel prices, and increasing power consumption, wind power is currently the world's fastest-growing electricity source. One essential form of renewable energy generation is wind energy conversion using a Doubly Fed Induction Generator (DFIG). Moreover, DFIGs are the best option, as wind turbines with variable speeds often have substantial megawatt capacity. Their cost-effectiveness, high operational efficiency, adaptable control mechanisms, and capacity to autonomously regulate the exchange of active and reactive power are the reasons for this selection. Classical control, which is based on PI regulators and employs several loops, is the most popular control approach that makes use of the indirect field-oriented vector method. In order to ensure stability across the whole speed range, it also requires strict regulation and is highly dependent on the correctness of the machine parameters. This paper presents a comparison between the classical PI and the metaheuristic Genetic Algorithm (GA), aiming to enhance the power extraction of DFIG under varying wind conditions. The simulation was carried out using MATLAB-SIMULINK, enabling the exploration of its performance across a range of operational scenarios. The results indicate that the PI controller optimized by GA demonstrates significant improvements over traditional controllers, particularly noted for its simplicity, faster convergence, and greater efficiency in power management.

Document Citation:

S. Heroual, B. Belabbas, K. Ayati, R. Haloui, A. T. Hassan, A. Ma'arif, M. M. Mahmoud, and V. Blazek, "Genetic Algorithm Tuned Controllers for High-Performance Indirect Field-Oriented Control in DFIG-Based WECS," *Buletin Ilmiah Sarjana Teknik Elektro*, vol. 8, no. 1, pp. 294-310, 2026, DOI: 10.12928/biste.v8i1.15529.

1. INTRODUCTION

Power-generation technologies have evolved to meet the 21st century's increasing need for power, which is mostly driven by fast population expansion and urbanization. The spike in demand has resulted in a global electrical shortfall [1][2]. To address these difficulties, power generation systems are typically divided into two categories: RESs, which are sustainable, and non-RESs, which are finite. This paradox mirrors the greater discussion over energy sustainability and resource management in modern society [3][4]. The development of RESs, which include geothermal, biomass, wind, solar, marine, and hydroelectric power, is the greatest way to preserve the environment and lessen pollution from fossil fuels and nuclear power [5][6]. The most sustainable, efficient, and promising of these energy sources is WE, which is one of the renewable energies that has seen a growth in use in the world due to its clean and non-polluting nature, which produces power without emitting greenhouse gases and is gradually being included in electrical networks [7]-[9].

By 2030, leading nations aim to produce over 20% of their electricity from WECS, according to recent research [10][11]. Nowadays, the most widely used WT in WFs is based on a DFIG because have special qualities, which include flexible control, low cost, high efficiency, and the potential to independently regulate the interchange of active and reactive electricity with the grid system [12]-[14]. Also, improved flexibility in the controllability of power factor by preserving the modest size of power electric devices [15]-[17].

The power output of a WECS is determined by the accuracy with which the peak power points are recorded by the MPPT controller of the WECS control system, regardless of the generator type employed at any wind speed [12],[18][19]. Due to the high degree of nonlinearity in the DFIG system, some control techniques have been considered to enhance the system's operation during disruptions. The most popular control using the FOVC method is classical control. This control strategy uses a variety of loops, heavily relies on the precision of the machine parameters, and requires strong regulation to maintain stability across the entire speed range, which is based on PI correctors [7],[20][21]. It is widely used due to its dependability and ease of implementation, but its effectiveness suffers when the internal generator parameters are changed [22][23]. Recent advances in non-linear control methods have had a significant impact on the control mechanisms of converters used in RESs, particularly solar and WT applications. These non-linear control approaches are distinguished by their high robustness in the face of disturbances and capacity to deal with the complex problems given by non-linear systems. As a result, they serve as useful instruments that not only meet the stringent standards of sustainable energy applications but also provide answers to typical problems associated with traditional linear PID control systems [21].

Several MPPT and control techniques of DFIG have been proposed in the literature to improve the performance and efficiency of WECS connected with DFIG [24]-[27]. In [28], the sliding mode regulator's decoupling control of active and reactive DFIG powers, which exhibits superiority over PI during robustness testing, unfortunately, this approach has a slow reaction time. Ref. [29] presents a comparison between PI and backstepping controllers for DFIGs used in WECSs. Its main objective was to assess the suggested controller's resilience against changes in wind speed and reference tracking. In [30], a PI gain based on a Fuzzy logic scheduler for a vector controller to regulate a DFIG utilized in a variable speed WT for wind power generation, but has the sensitivity to changes in parameters and outside disturbances. In [31], various control strategies for DFIG-WECS using RST and fuzzy logic controllers were found, where the first control is more robust than the novel control compared to the rotor resistance variation, but the oscillations remain apparent. In [32], DFIG connected to a WT controlled by a novel DTC using the rotor power factor by maintaining it equal to one, and rotor voltage vectors produced by utilizing a look-up table it has a great reduction of torque ripples but has a complex structure in control. In [33], a hybrid algorithm (PSO and GSA) was used to optimize a fuzzy sliding mode controller. The major drawback of these techniques is the complexity of the synthesis process, and it needs the full knowledge of system parameters and boundaries. In [34], using the DFIG's backstepping adaptive control for variable-speed WTs utilizes an adaptive pole placement technique.

This work provides a thorough comparison of classic optimization methods with a novel meta-heuristic methodology known as the GA. This study focuses on optimizing the k_p and k_i parameters of the PI regulator, which is utilized in WECS and in conjunction with DFIGUREThe primary purpose of this optimization work is to increase the system's ability to track wind speed accurately, which is critical for maximizing the power output generated by WE systems. Furthermore, the analysis emphasizes the need to improve the dynamic damping performance of the associated machines, arguing that the GA may provide more effective solutions than standard methods for achieving these goals.

The paper describes the framework of the work, which is divided into six sections. Section 2 focuses on the DFIG-based WECS, including system and inverter specifications. Section 3 describes the control technique that includes MPPT, field-oriented vector control, and PWM control methodologies. Section 4 introduces the

suggested GA, while Section 5 presents simulation results and debates. Section 6 present conclusion that closes the work.

2. MODELLING OF WECS COMPONENTS

2.1. WT Model (WTM)

Figure 1 shows a block schematic of the turbine's dynamic model [35]-[37]. The mechanical power transmitted from the wind to the aerodynamic rotor is defined as [38]-[41]:

$$P_a = C_p(\lambda,\beta).P_v = \frac{1}{2}C_p(\lambda,\beta)\rho.\pi.R^2.v^3 \quad (1)$$

The input torque aerodynamic:

$$\mathrm{T_m} = \frac{\mathrm{P_m}}{\Omega_\mathrm{t}} \quad (2)$$

The gearbox model is:

$$\Omega_\mathrm{t} = \frac{1}{G}\Omega_\mathrm{mec} \quad (3)$$

$$\mathrm{T_{mg}} = \frac{1}{G}T_\mathrm{m} \quad (4)$$

The shaft model is:

$$\mathrm{J}.\frac{\mathrm{d}\Omega_\mathrm{m}}{\mathrm{dt}} = \mathrm{T_m} - \mathrm{T_g} \quad (5)$$

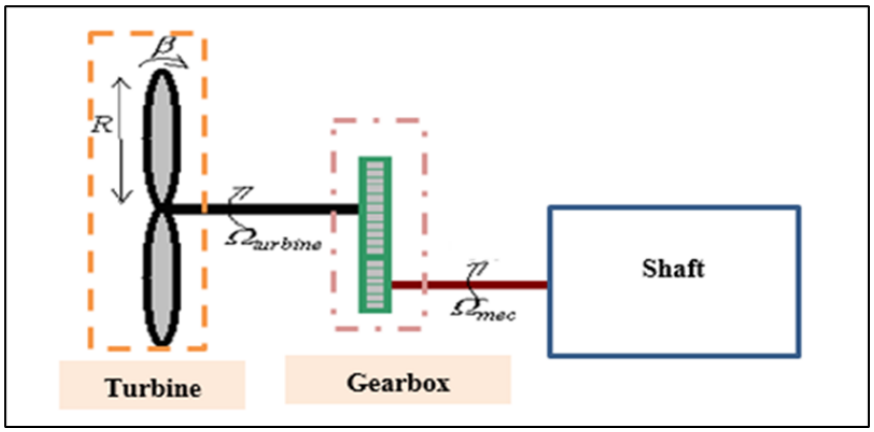

Figure 1. Model of the turbine [35]

2.2. DFIG Model

Figure 2 shows Park's transformation and the two-phase reference model of the wound rotor induction machine in the rotating field reference frame [42]. The formulae for the stator and rotor voltages are as follows [43]-[45]:

$$\begin{cases} V_{sd} = R_s i_{sd} + \dfrac{d}{dt}\phi_{sd} - \omega_s\phi_{sq} \\ V_{sq} = R_s i_{sq} + \dfrac{d}{dt}\phi_{sq} + \omega_s\phi_{sd} \\ V_{rd} = R_r i_{rd} + \dfrac{d}{dt}\phi_{rd} - \phi_{rq} \\ V_{rq} = R_r i_{rq} + \dfrac{d}{dt}\phi_{rq} + \omega_s\phi_{rd} \end{cases} \quad (6)$$

The formulae for the stator and rotor flux are as follows:

$$\begin{cases} \Phi_{sd} = L_s i_{sd} + M_{sr} i_{rd} \\ \phi_{sq} = L_s i_{sq} + M_{sr} i_{rq} \\ \phi_{rd} = L_r i_{rd} + M_{sr} i_{sd} \\ \phi_{rq} = L_r i_{rq} + M_{sr} i_{sq} \end{cases} \quad (7)$$

The equation between stator and rotor pulsations and rotor speed is as outlined below:

$$\omega_s = \omega + \omega_r \quad (8)$$

The torque formulae of the DFIG are:

$$T_{em} = p \frac{M_{sr}}{L_s} \left(\phi_{sq} i_{rd} - \phi_{sd} i_{rq} \right) \quad (9)$$

The equations for the stator and rotor powers are as follows:

$$\begin{cases} P_s = V_{sd} i_{sd} + V_{sq} i_{sq} \\ Q_s = V_{sq} i_{sd} - V_{sd} i_{sq} \end{cases} \quad (10)$$

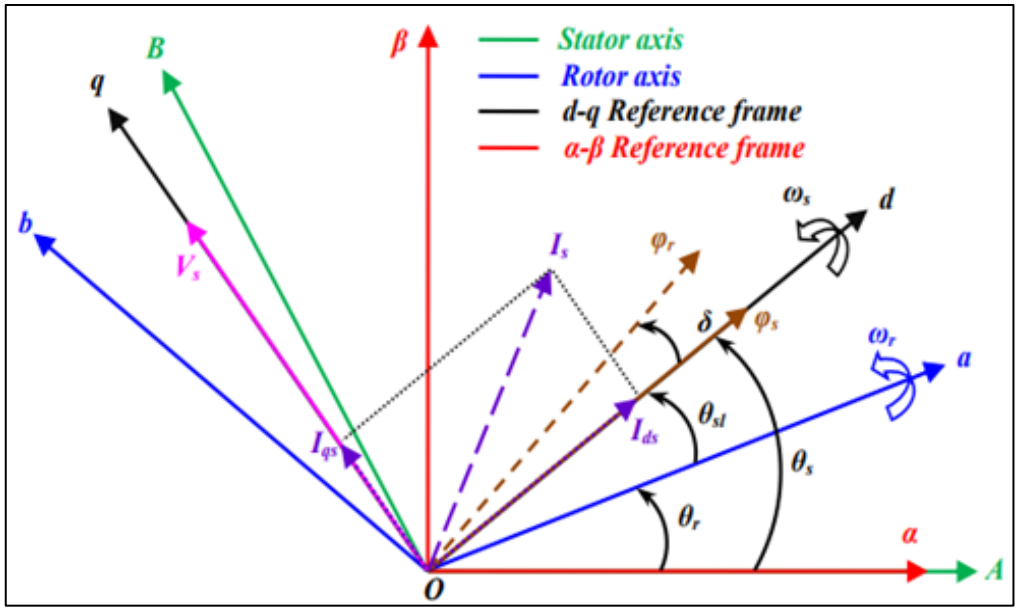

Figure 2. Orientation of the park frame [42]

2.3. Three-Level NPC Inverter

The three-level NPC, developed by Nabae *et al*., consists of four switches in each leg and two diodes clamped to the capacitors' midpoints and composed of four IGBT switches. The controlled switches are unidirectional in voltage and bidirectional in current, as depicted in Figure 3 [46]-[48]. Table 1 shows the three-level NPC inverter switch states based on the output voltage. Sequence positive: The switches S_{a1}, S_{a2} are opened, and S_{a3}, S_{a4} are closed. The output voltage equals $E/2$. Sequence zero: The switches S_{a2} ,$S_{a3}$are opened, and S_{a1}, S_{a4} are closed. The output voltage equals 0. Sequence negative: The switches S_{a1}, S_{a2} are closed and S_{a3},S_{a4} are opened. The output voltage equals $-E/2$ [43].

Table 1. Switching state of the three-level NPC inverter [24].

Sequence	S_{a1}	S_{a2}	S_{a3}	S_{a4}	Output
Positive	1	1	0	0	$E/2$
Zero	0	1	1	0	0
Negative	0	0	1	1	$-E/2$

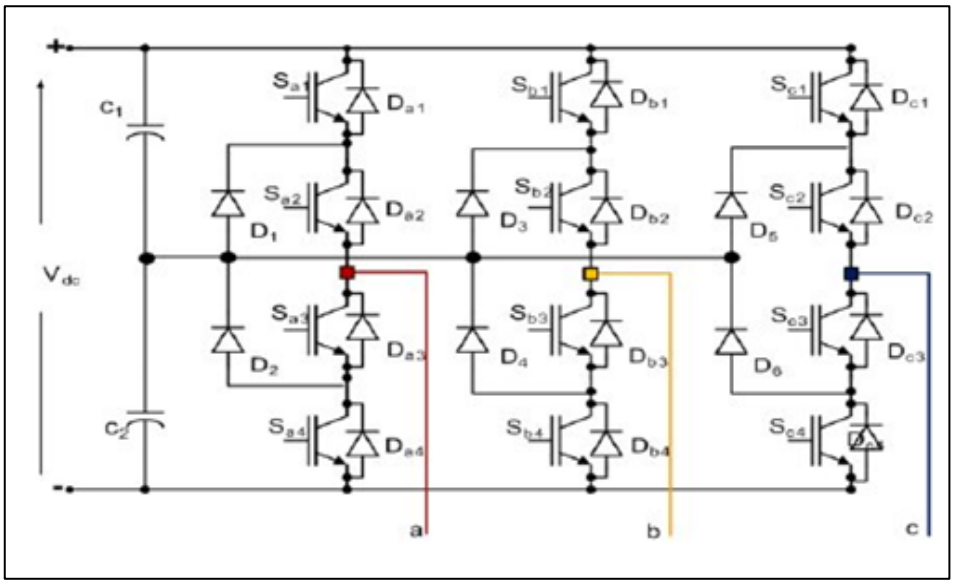

Figure 3. Topology of NPC inverter [47]

3. CONTROL OF WIND-DRIVEN DFIG

3.1. MPPT Model

WE fluctuate's with wind speed throughout the day. The quantity of power delivered by a WECS depends on the MPPT controller's accuracy in tracking peak power points, independent of generator type [13],[49]. The power coefficient in equation (1) depends on both the blade pitch angle β and the tip-speed ratio λ. This work utilizes a fixed pitch angle $\beta = 0$, indicated $(\lambda_{opt} = 8.1,) = 0.48)$, which is the point corresponding to the maximum of the mechanical power recovered as depicted in Figure 4. The tip-speed ratio optimal is determined by [35],[50]:

$$\lambda_{\text{opt}} = \frac{\text{R}.\,\Omega_{\text{opt}}}{\text{v}} \tag{11}$$

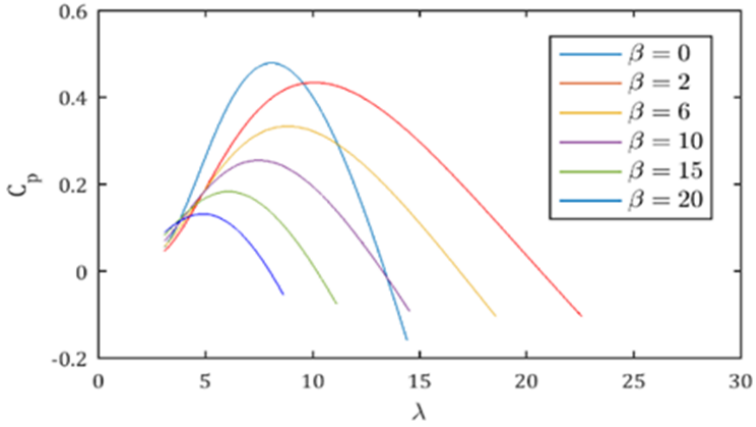

Figure 4. Cp versus λ

Figure 5 shows the control design that uses a classical *PI* controller to calculate electromagnetic reference torque based on the difference between reference and rotation speeds. The coefficients K_{p} and K_{I} regulators are calculated as (12) and (13):

$$K_{\text{p}} = \frac{J}{\tau} \tag{12}$$

$$K_I = \frac{F}{\tau} \tag{13}$$

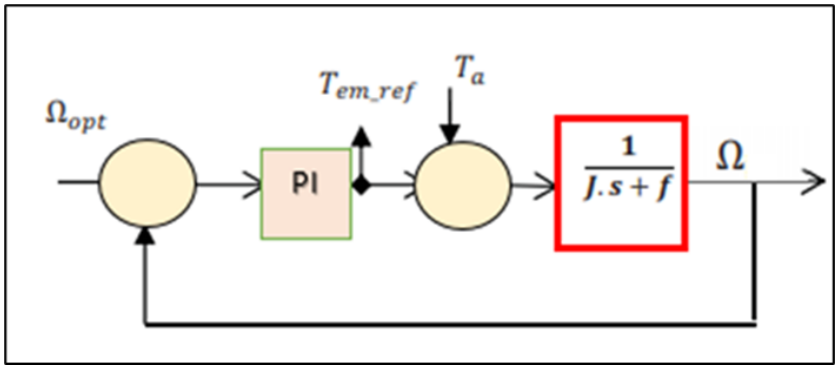

Figure 5. Block diagram of speed controls

3.2. Field-Oriented Vector Control

The method of vector control is intended to achieve the decoupling between flow control and electromagnetic torque [51][52]. The modeling of the DFIG with a stator field-oriented [53]-[55]. A simplified expression of the electromagnetic torque is obtained by setting the following conditions:

$$\begin{aligned} \phi_{sd} &= \phi_s \\ \phi_{sq} &= 0 \end{aligned} \tag{14}$$

Equation systems can be simplified as follows:

$$\begin{cases} V_{sd} = R_s i_{sd} \\ V_{sq} = R_s i_{sq} + \omega_s \phi_s \\ V_{rd} = R_r i_{rd} + \dfrac{d\phi_{rd}}{dt} - \omega_r \phi_{rq} \\ V_{rq} = R_r i_{rq} + \dfrac{d\phi_{rq}}{dt} + \omega_r \phi_{rd} \end{cases} \tag{15}$$

The voltage and flux equations of the stator windings may be streamlined in a steady state as follows, assuming that the resistance of the stator winding R_s is neglected.

$$\begin{cases} V_{sd} = 0 \\ V_{sq} = V_s = \omega_s \phi_s \\ V_{rd} = R_r i_{rd} + \dfrac{d\phi_{rd}}{dt} - \omega_r \phi_{rq} \\ V_{rq} = R_r i_{rq} + \dfrac{d\phi_{rq}}{dt} + \omega_r \phi_{rd} \end{cases} \tag{16}$$

The torque formulae of the flux:

$$\begin{cases} \Phi_s = L_s i_{sd} + M_{sr} i_{rd} \\ 0 = L_s i_{sq} + M_{sr} i_{rq} \\ \phi_{rd} = L_r i_{rd} + M_{sr} i_{sd} \\ \phi_{rq} = L_r i_{rq} + M_{sr} i_{sq} \end{cases} \tag{17}$$

The electromagnetic torque expression is:

$$T_{em} = -P \frac{M_{sr}}{L_s} \phi_s i_{rq} \tag{18}$$

The active and reactive stator powers are as outlined (19):

$$\begin{aligned} P &= V_s i_{sq} \\ Q &= V_s i_{sd} \end{aligned} \tag{19}$$

The equations related between the stator and the rotor currents are calculated (20):

$$\begin{cases} I_{sd} = \dfrac{V_s}{\omega_s L_s} - \dfrac{M_{sr}}{L_s} i_{rd} \\ i_{sq} = -\dfrac{M_{sr}}{L_s} i_{rq} \end{cases} \tag{20}$$

By replacing the direct and quadrature stator currents with their expressions in the equations of active and reactive powers:

$$\begin{cases} P = -\dfrac{V_s M_{sr}}{L_s} i_{rq} \\ Q = -\dfrac{V_s M_{sr}}{L_s} i_{rd} + \dfrac{{V_s}^2}{\omega_s L_s} \end{cases} \tag{21}$$

To ensure appropriate machine management, it's necessary to determine the relation between the rotor voltages and currents supplied to the machine [51].

$$\begin{cases} \Phi_{rd} = \left(L_r - \dfrac{{M_{sr}}^2}{L_s}\right) i_{rd} - \dfrac{M_{sr} V_s}{\omega_s L_s} \\ \phi_{rq} = \left(L_r - \dfrac{{M_{sr}}^2}{L_s}\right) i_{rq} \end{cases} \tag{22}$$

The equation of the voltage rotor:

$$\begin{cases} V_{rd} = R_r i_{rd} + \left(L_r - \dfrac{{M_{sr}}^2}{L_s}\right) \dfrac{di_{rd}}{dt} - g\omega_s \left(L_r - \dfrac{{M_{sr}}^2}{L_s}\right) i_{rq} \\ V_{rq} = R_r i_{rq} + \left(L_r - \dfrac{{M_{sr}}^2}{L_s}\right) \dfrac{di_{rq}}{dt} - g\omega_s \left(L_r - \dfrac{{M_{sr}}^2}{L_s}\right) i_{rd} + g\dfrac{M_{sr} V_s}{L_s} \end{cases} \tag{23}$$

In a steady regime, the equation will be as follows:

$$\begin{cases} V_{rd} = R_r i_{rd} - g\omega_s \left(L_r - \dfrac{{M_{sr}}^2}{L_s}\right) i_{rq} \\ V_{rq} = R_r i_{rq} - g\omega_s \left(L_r - \dfrac{{M_{sr}}^2}{L_s}\right) i_{rd} + g\dfrac{M_{sr} V_s}{L_s} \end{cases} \tag{24}$$

The field vector indirect control without and with power control is presented in Figure 6 and Figure 7, respectively [54]. The design of a conventional PI regulator for controlling currents i_{rd} and i_{rq} is seen in Figure 8.

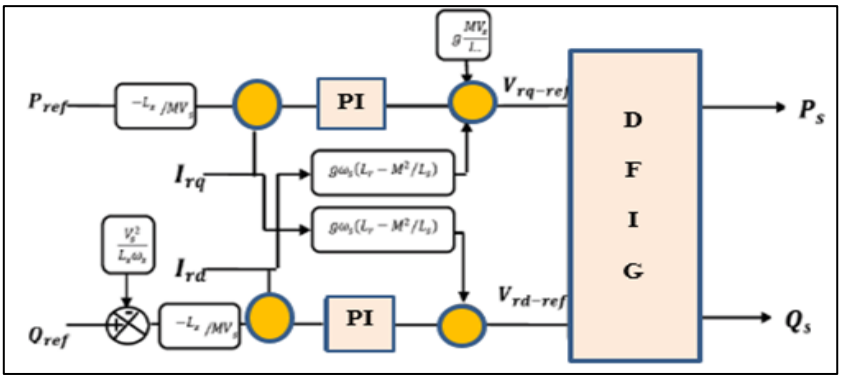

Figure 6. Block diagram of FOPI without power control [54]

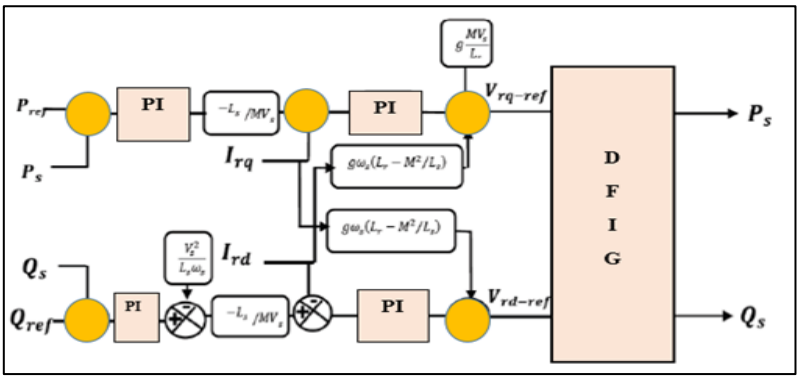

Figure 7. Block diagram of FOPI with power control [54]

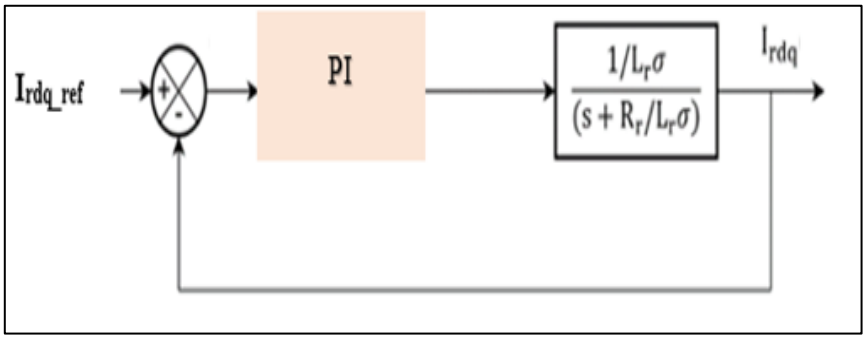

Figure 8. Block diagram of current controls

The coefficients K_p and K_i regulators are calculated as (25) and (26):

$$K_{Pi\_rd} = \frac{L_r \cdot \sigma}{\tau_1} \tag{25}$$

$$K_{Pi\_irq} = \frac{R_r}{\tau_1} \tag{26}$$

The design of the PI for controlling currents P_{ms}, Q_{ms} is depicted in Figure 9. The coefficients K_p and K_i regulators are calculated as (27) and (28):

$$K_{P(P_{mes},Q_{mes})} = \frac{L_r \cdot \sigma}{\tau_2 \cdot K_{Pirdq}} \tag{27}$$

$$K_{i(P_{mes},Q_{mes})} = \frac{1}{\tau_2} \tag{28}$$

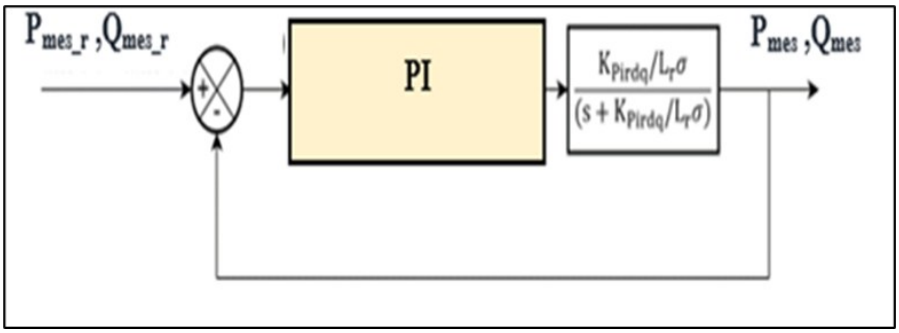

Figure 9. Block diagram of power controls

3.3. Three-Level Sinusoidal Pulse Width Modulation Strategy

The three-level sine-based PWM inverter works on the same principles as a two-level inverter. The key mechanism in its operation is producing sine carrier PWM by comparing two triangular carrier waves to three unique reference control signals. This method provides for greater control and modification of the output voltage, resulting in higher performance in a variety of situations where PWM inverters are used. The inverter gate devices are to receive the matching pulses that are created. The three reference control signals are phase shifts by an angle of $2\pi/3$ and $4\pi/3$ with the same amplitude. With a DC voltage offset, two carrier waves are in phase with one another. For three-phase SPWM [56][57]:

$$V_{peak} = \mathrm{m}\ \frac{V_{dc}}{2} \tag{29}$$

3.4. Genetic Algorithm

GA falls within the category of evolutionary algorithms. Holland first laid out the basic ideas of GA [58]. They aim to find an approximate solution to an optimization issue. GA employs probabilistic transition rules to handle a population of possible solutions, called individuals or chromosomes, which evolve repeatedly [59] [60]. Each iteration of the algorithm is called a generation. Solution evolution is simulated using a fitness function and genetic operators, including reproduction, crossover, and mutation [61]. The GA steps are as follows:

a) Initial Population

The algorithm starts by creating arbitrary primary inhabitants. In MATLAB, the main population typically consists of 35 entities, indicating an evasion rate of the population range [62]. One of the most common initialization techniques is the use of random binary characters, as depicted in Figure 10.

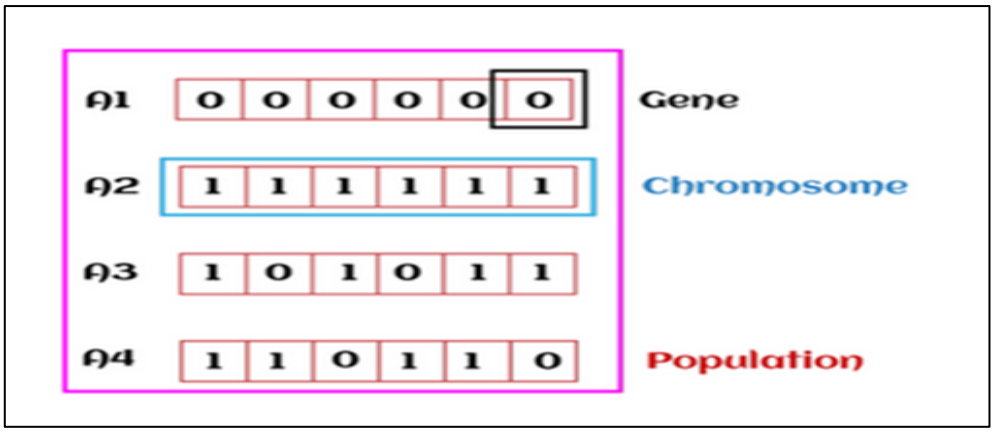

Figure 10. Initialization strategy

b) Function fitness

This alludes to an individual's capacity to compete against others. Individuals are scored on their fitness function in each iteration. Each person obtains a fitness score from the fitness function. This score also affects your chances of getting picked for reproduction. The greater the fitness score, the more probable that the individual will be chosen for reproduction [63]. The GA uses present residents to generate children for future generations. The algorithm selects parents from the present population to pass on their genes to their children. The GA often chooses entities with high vigor rates, such as parents [60][61]. The GA creates three sorts of children for the following generation:

c) Selection

During the selection stage, individuals are chosen for progeny reproduction. Every one of the chosen individuals is placed in pairs of two to improve reproduction. The following generation subsequently inherits these people's DNA [61].

d) Crossover

Crossover offspring are created by combining the vectors of a pair of parents from the current population. The evasion intersect task randomly selects a gene from one of the two parents and assigns it to the kid vector at each iteration [60].

e) Mutation

To maintain population diversity, the mutation operator transfers random genes into the offspring (new child). This can be accomplished by shifting a few chromosomal bits. Thus, mutation solves the problem of early convergence and increases diversity [61][62]. In this work, the GA is used to optimize the parameters of the conventional PI regulator in DFIG and WECS.

The following are the Genetic algorithm steps for tuning the parameters of the PI regulator, followed with flowchart depicted in Figure 11:

- The transfer function should be introduced.
- Create a random Nchromosome population $[a\ b]$.
- **Fitness:** Assess each population's chromosome X's objective function ITAE.
- New population: create a new population, repeat the steps below until it is complete:
  - **Select** two parent chromosomes, K_p and K_i, from a population based on their ITAE fitness.
  - **Crossover:** With a crossover chance, the parents will cross to produce new offspring. If no crossover were conducted, the offspring would be a replica of the parents.
  - **Mutation:** With a mutation chance, create new offspring at each locus.
- **Accepting:** Add new offspring to the new populations K_p and K_i
- **Replace**: Rerun the algorithm using the freshly created population.
- To stop the process, obtain the optimal parameters gain $K_p\ and\ K_i$
- Check if the end condition is met. Go back to step 3.

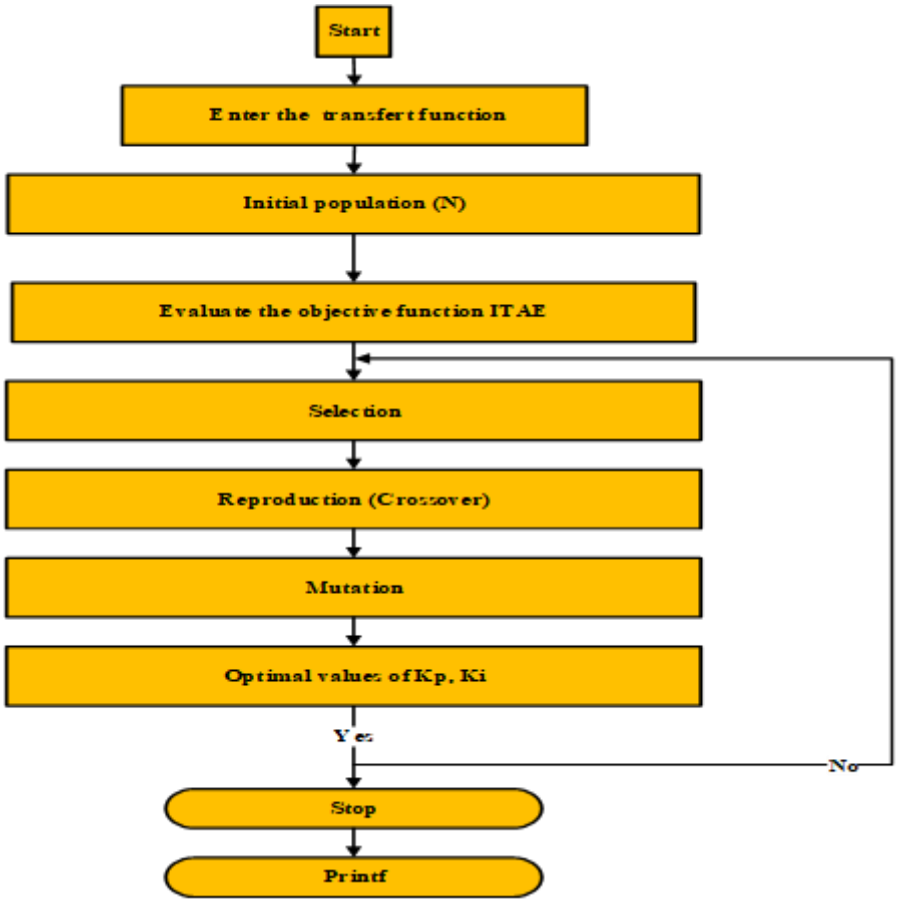

Figure 11. Flowchart of GA

4. SIMULATED RESULTS AND DISCUSSIONS

The suggested methodology was validated by thorough testing of a DFIG-based WECS in Simulink/MATLAB. This validation carefully investigates the system's performance under changing wind speeds, particularly between 7.6 and 8.4, as shown in Figure 12. Several simulations were carried out to better

understand the differences between the various suggested controllers used in MPPT for maximizing power extraction from WECS. The simulation results shown in Figure 13 show a clear link between mechanical speed and reference speed. The results support the usefulness of the genetic algorithm used, demonstrating its capacity to provide a quick reaction while reducing overshoot. This high performance is critical since it helps to maximize power production.

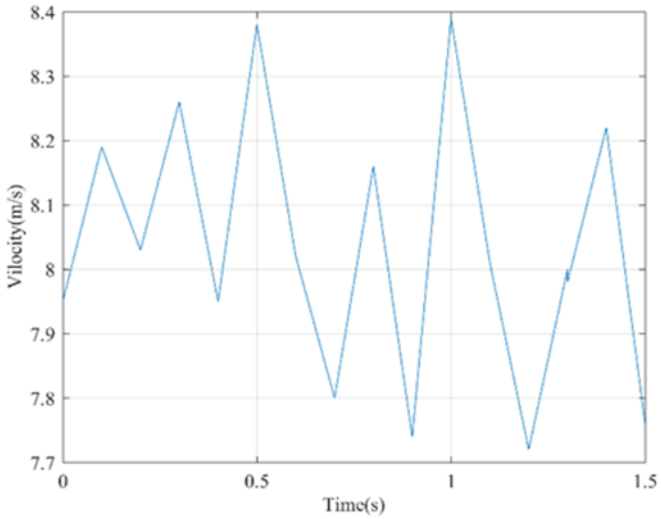

Figure 12. Wind input

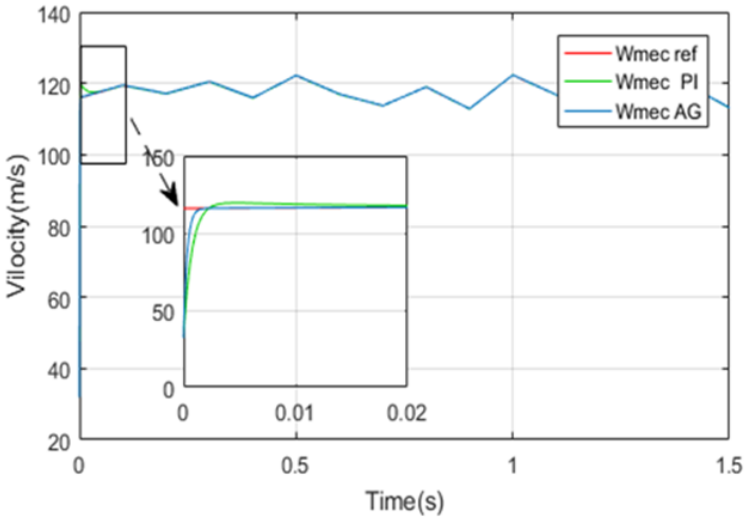

Figure 13. Turbine wind speed obtained by PI and GA

The graphic depicted in Figure 14 and Figure 15 compares the d-q rotor current responses of a DFIG under two control strategies: the Pole Placement controller and the GA controller. During a 0.5 $second$, the d-axis rotor current demonstrates that both controllers are in operation, the PP controller exhibits greater variations, whilst the GA controller has a smoother, better-damped response. The q-axis rotor current has a transient. At 0.5 s and a step change at 1 s, with the PI controller providing a gentle transition, reacting lower with more fluctuations. The PI controller thus provides better dampening and smoother dynamics, whereas the AG controller allows for faster response at the expense of harsher transients. According to the analysis, the GA approach outperforms the PP method in terms of response characteristics and dynamics. Figure 16 and Figure 17 exhibit the machine's effective decoupling, emphasizing the relevance of the FOCI in power regulation. The research shows that the pole placement method generates gain values that result in inferior performance, particularly when system gains fluctuate, highlighting its shortcomings. In contrast, the GA optimization method produces superior outcomes, demonstrating excellent stability and dynamic performance in the face of

change. The data strongly show that GA optimization outperforms pole placement in terms of delivering stable and efficient power regulation while avoiding the introduction of major dynamic faults.

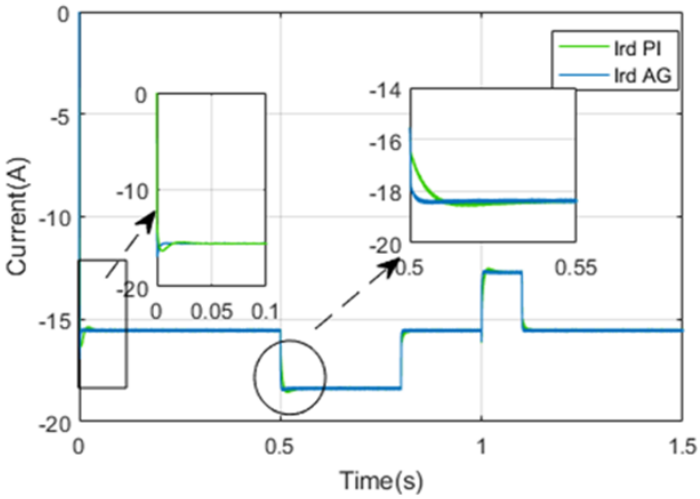

Figure 14. DFIG rotor current direct

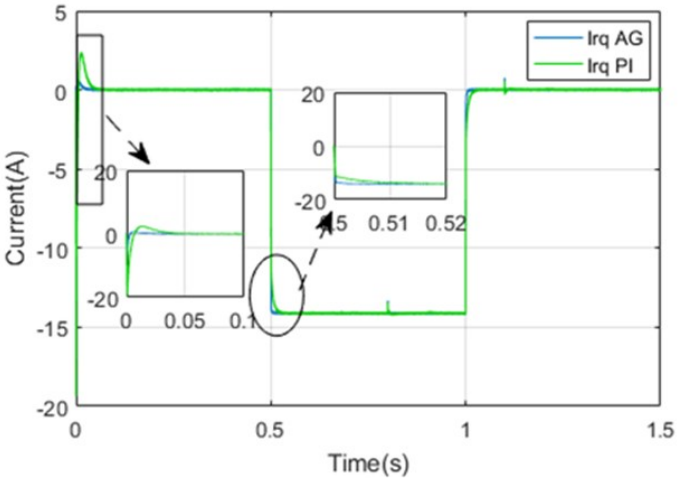

Figure 15. DFIG rotor current quadrature

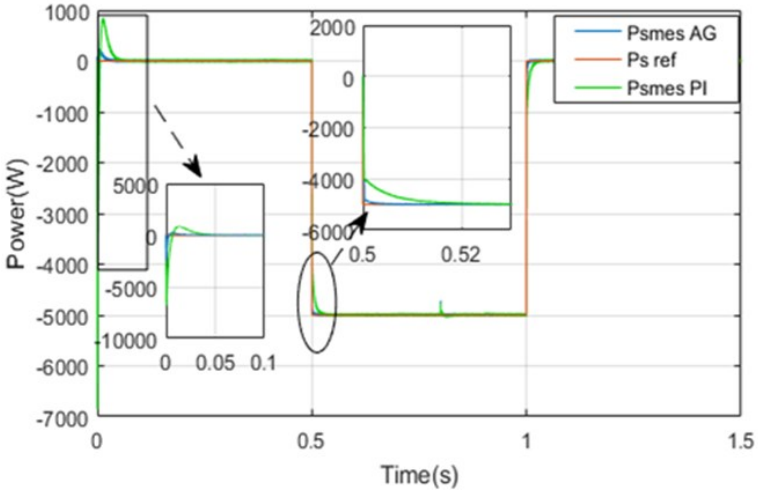

Figure 16. Active power

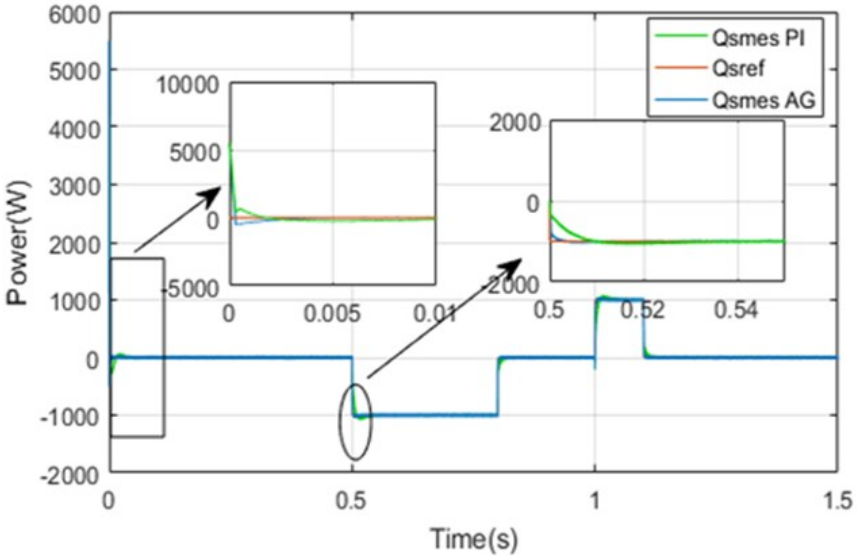

Figure 17. Reactive power

Table 2 and Table 3 compare the PI controller gains obtained by two different methods: pole placement and genetic algorithm optimization. The Table 1 shows that the pole placement method gives much larger gains ($k_p = 98.90, k_i = 163$) compared to the genetic algorithm method ($k_p = 54.30, k_i = 102$), which indicates a stronger control action but makes the control system less sensitive to disturbances. Table 3 emphasizes the current and power control loops, where the same conclusion is drawn, indicating that the pole placement method always gives larger gains in both cases. This indicates that the pole placement method favors fast response and accuracy in tracking, while the genetic algorithm method favors a stable and moderate control action.

Table 2. PI controller gains speed controls.

Methods	k_p	k_i
Pole placement	98.90	163
Genetic algorithm	54.30	102

Table 3. PI gains currents and powers controls.

Methods		k_p	k_i
Pole placement	currents	12.85	930
Pole placement	power	11.16	4545.5
Genetic algorithm	currents	5.90	734
Genetic algorithm	power	5.34	4291

5. CONCLUSIONS

This paper introduces a WECS using a DFIG, with emphasis on the construction of a global model and a vector control scheme aimed at controlling the active and reactive power outputs of the DFIGUREThe control scheme uses PI control with the addition of a genetic algorithm for optimization, particularly in MPPT and FOC. Among the major findings of this research work is that the use of PI control with variable parameters (PI-PP) results in better performance with lower settling times and over-peak overshoots, culminating in a faster stabilization process. On the other hand, the use of genetic algorithm-optimized PI control shows greatly improved convergence speeds to the gain values and better transient response characteristics compared to traditional PI control schemes. This improvement is critical in ensuring that the DFIG system performs well even at high power levels, ultimately providing better performance and stability. The paper recognizes some limitations, which open avenues for future research, especially in the area of adaptive methodologies. It is postulated that hybrid approaches may be used to improve dynamic behavior. Such advances may help to improve the efficiency and scalability of GA and extend its applications to different areas, such as real-time control systems and machine learning. The paper also stresses the need to validate the present findings by comparing them with the results of virtual simulations and real-time experimental results.

Appendix

Table 4. DFIG Parameters

Stator frequency f	50Hz
Stator rated voltage Vs Rated	220V/380V
Pair of poles P	2
Stator resistance Rs	0.455Ω
Rotor resistance Rr	0.62Ω
Statoric inductance Ls	0.084H
Rotoric inductance Lr	0.081H
Mutual inductance Msr	0.078H
Moment of inertia Fg	0.3125 Kg. m ^{2}
Coefficient of friction	$6.73.10^{-3}$ N. m. s^{-1}

Table 5. Wind Turbine Parameters

Blade's radius R	3
Gain of gearboxε G	5.4
Air density ρ	1.225 kg/m3
Moment of inertia turbine	3.1959Kg. m^2
Coefficient of friction of a turbine	0.0073 N. m. s^{-1}

List of Abbreviations

MPPT: Maximum Power Point Tracking	PI: proportional-integral
DFIG: Doubly Fed Induction Generator	GA: genetic algorithm
WECS: wind energy conversion system	WTs: wind turbines
IFOVC: indirect field-oriented vector method	RESs: renewable energy systems
WE: wind energy	WFs: wind farms
DTC: direct torque control	PWM: Pulse Width Modulation
FOCI: Flexible Operation Control Interface	

Declaration

Author Contribution

All authors contributed equally to the main contributor to this paper. All authors read and approved the final paper.

Acknowledgment

This article has been produced with the financial support of the European Union under the REFRESH-Research Excellence for REgion Sustainability and High-tech Industries project number CZ.10.03.01/00/22_003/0000048 via the Operational Programme Just Transition.

Conflicts of Interest

The authors declare no conflict of interest.

REFERENCES

[1] M. Tarek and M. I. M. Elzein, "Sustainable Energy Management in Islanded Microgrids via HHO – BE Tuned Adaptive Controllers and Demand-Side Flexibility," *Eng. Reports*, vol. 8, no. 1, pp. 1–20, 2026, https://doi.org/10.1002/eng2.70561.

[2] S. Nadweh and M. M. M. , I. M. Elzein, Daniel Eutyche Mbadjoun Wapet, "Optimizing control of single- ended primary inductor converter integrated with microinverter for PV systems : Imperialist competitive algorithm," *Energy Explor. Exploit.*, vol. 44, no. 1, pp. 554-577, 2026, https://doi.org/10.1177/01445987251382002.

[3] J. Mwaniki, H. Lin, and Z. Dai, "A Condensed Introduction to the Doubly Fed Induction Generator Wind Energy Conversion Systems," *Journal of Engineering (United Kingdom)*, vol. 2017, no. 1, p. 2918281, 2017, https://doi.org/10.1155/2017/2918281.

[4] D. Cui *et al.*, "Enhancing Short-Term Electricity Forecasting with Advanced Machine Learning Techniques," *J. Electr. Eng. Technol.*, vol. 21, no. 1, pp. 147-187, 2026, https://doi.org/10.1007/s42835-025-02430-z.

[5] G. S. Kaloi, J. Wang, and M. H. Baloch, "Active and reactive power control of the doubly fed induction generator based on wind energy conversion system," *Energy Reports*, vol. 2, pp. 194–200, 2016, https://doi.org/10.1016/j.egyr.2016.08.001.

[6] M. Basu *et al.*, "Flexible Dynamic Optimal Power Flow Integrating Renewable Energy Sources and Electric Vehicle Parking IOT," *Eng. Reports*, vol. 7, no. 12, 2025, https://doi.org/10.1002/eng2.70568.

[7] R. D. Shukla and R. K. Tripathi, "A novel voltage and frequency controller for standalone DFIG based Wind Energy Conversion System," *Renewable and Sustainable Energy Reviews*, vol. 37. pp. 69–89, 2014, https://doi.org/10.1016/j.rser.2014.04.069.

[8] N. V. A. Ravikumar *et al.*, "Design and real-time simulations of robust controllers for uncertain multi-input wind turbine," *Energy Explor. Exploit.*, vol. 44, no. 1, pp. 276-292, 2026, https://doi.org/10.1177/01445987251373101.
[9] S. Basu *et al.*, "Applications of Snow Ablation Optimizer for Sustainable Dynamic Dispatch of Power and Natural Gas Assimilating Multiple Clean Energy Sources," *Eng. Reports*, vol. 7, no. 6, pp. 1–12, 2025, https://doi.org/10.1002/eng2.70211.
[10] S. Boubzizi, H. Abid, A. El hajjaji, and M. Chaabane, "Comparative study of three types of controllers for DFIG in wind energy conversion system," *Prot. Control Mod. Power Syst.*, vol. 3, no. 1, 2018, https://doi.org/10.1186/s41601-018-0096-y.
[11] N. F. Ibrahim, I. M. Elzein, M. M. Mahmoud, A. M. El-Rifaie, H. S. Hussein, and M. A. E. Eid, "Enhanced Control of Single-Stage PV-STATCOM Using Hybrid MPPT and Adaptive AHLMS for Power Quality Improvement," *IEEE Access*, vol. 13, pp. 200253–200270, 2025, https://doi.org/10.1109/ACCESS.2025.3635707.
[12] H. Chojaa *et al.*, "Nonlinear Control Strategies for Enhancing the Performance of DFIG-Based WECS under a Real Wind Profile," *Energies*, vol. 15, no. 18, 2022, https://doi.org/10.3390/en15186650.
[13] S. Saeed, R. Asghar, F. Mehmood, H. Saleem, B. Azeem, and Z. Ullah, "Evaluating a Hybrid Circuit Topology for Fault-Ride through in DFIG-Based Wind Turbines," *Sensors*, vol. 22, no. 23, 2022, https://doi.org/10.3390/s22239314.
[14] W. Fendzi *et al.*, "Policy-driven expansion of renewable energy in Cameroon : A technical and sustainability-centered analysis of growth trends and cross-sectoral impacts (2015 – 2024)," *Energy Strateg. Rev.*, vol. 62, p. 101912, 2025, https://doi.org/10.1016/j.esr.2025.101912.
[15] H. Liu, S. Yang, and X. Yuan, "Inertia control strategy of DFIG-based wind turbines considering low-frequency oscillation suppression," *Energies*, vol. 15, no. 1, 2022, https://doi.org/10.3390/en15010029.
[16] H. Abdelfattah, I. Elzein, M. M. Mahmoud, M. I. Mosaad, W. Fendzi Mbasso, and N. F. Ibrahim, "Supporting the reactivity of nuclear power plants using an optimized FOPID controller with arithmetic algorithm: Toward an environmentally sustainable energy system," *Energy Explor. Exploit.*, vol. 43, no. 6, pp. 2446-2472, 2025, https://doi.org/10.1177/01445987251357362.
[17] A. Hysa, S. Sefa, I. M. Elzein, A. Ma, M. M. Mahmoud, and E. Touti, "Advanced Modeling and Comparative Error Analysis of Photovoltaic Cells Using Multi-Diode Models and EQE Characterization," *J. Robot. Control*, vol. 6, no. 5, pp. 2308–2321, 2025, https://doi.org/10.18196/jrc.v6i5.27539.
[18] W. S. E. Abdellatif, A. M. Hamada, and S. A. M. Abdelwahab, "Wind speed estimation MPPT technique of DFIG-based wind turbines theoretical and experimental investigation," *Electr. Eng.*, vol. 103, no. 6, pp. 2769–2781, 2021, https://doi.org/10.1007/s00202-021-01268-8.
[19] I. M. Elzein, Y. Maamar, M. M. Mahmoud, M. I. Mosaad, and S. A. Shaaban, "The Utilization of a TSR-MPPT-Based Backstepping Controller and Speed Estimator Across Varying Intensities of Wind Speed Turbulence," *Int. J. Robot. Control Syst.*, vol. 5, no. 2, pp. 1315–1330, 2025, https://doi.org/10.31763/ijrcs.v5i2.1793.
[20] P. K. Dash and R. K. Patnaik, "Adaptive second order sliding mode control of doubly fed induction generator in wind energy conversion system," *J. Renew. Sustain. Energy*, vol. 6, no. 5, 2014, https://doi.org/10.1063/1.4899193.
[21] N. Dahri, M. Ouassaid and D. Yousfi, "A FOC Based Robust Fuzzy Logic Controller for a Wind Energy Conversion System to Overcome Mechanical Parameter Uncertainties," *2020 IEEE International Autumn Meeting on Power, Electronics and Computing (ROPEC)*, pp. 1-7, 2020. https://doi.org/10.1109/ROPEC50909.2020.9258772.
[22] U. Javed, M. A. Arshad, M. Jawad, N. Shabbir, L. Kutt, and A. Rassolkin, "Active and Reactive Power Control of DFIG using Optimized Fractional Order-PI Controller," in *Proceedings - 2021 IEEE 19th International Power Electronics and Motion Control Conference, PEMC 2021*, pp. 398–404, 2021, https://doi.org/10.1109/PEMC48073.2021.9432608.
[23] A. Fayz *et al.*, "Optimal Controller Design of Crowbar System for DFIG-based WT : Applications of Gravitational Search Algorithm," *Bul. Ilm. Sarj. Tek. Elektro*, vol. 7, no. 2, pp. 122–136, 2025, https://doi.org/10.12928/biste.v7i2.13027.
[24] T. Boutabba, I. Benlaloui, F. Mechnane, I. M. Elzein, M. Ammar, and M. M. Mahmoud, "Design of a Small Wind Turbine Emulator for Testing Power Converters Using dSPACE 1104," *Int. J. Robot. Control Syst.*, vol. 5, no. 2, pp. 698–712, 2025, https://doi.org/http://dx.doi.org/10.31763/ijrcs.v5i2.1685.
[25] O. Makram Kamel, I. M. Elzein, M. M. Mahmoud, A. Y. Abdelaziz, M. M. Hussein, and A. A. Zaki Diab, "Effective energy management strategy with a novel design of fuzzy logic and JAYA-based controllers in isolated DC/AC microgrids: A comparative analysis," *Wind Eng.*, vol. 49, no. 1, pp. 199–222, 2025, https://doi.org/10.1177/0309524X241263518.
[26] F. Menzri, T. Boutabba, I. Benlaloui, H. Bawayan, M. I. Mosaad, and M. M. Mahmoud, "Applications of hybrid SMC and FLC for augmentation of MPPT method in a wind-PV-battery configuration," *Wind Eng.*, vol. 48, no. 6, pp. 1186-1202, 2024, https://doi.org/10.1177/0309524X241254364.
[27] H. Boudjemai *et al.*, "Design, Simulation, and Experimental Validation of a New Fuzzy Logic-Based Maximal Power Point Tracking Strategy for Low Power Wind Turbines," *Int. J. Fuzzy Syst.*, vol. 5, no. 1, pp. 296–310, 2025, https://doi.org/10.31763/ijrcs.v5i1.1425.
[28] L. Djilali, E. N. Sanchez, and M. Belkheiri, "Real-time implementation of sliding-mode field-oriented control for a DFIG-based wind turbine," *Int. Trans. Electr. Energy Syst.*, vol. 28, no. 5, 2018, https://doi.org/10.1002/etep.2539.

[29] Z. Zeghdi, L. Barazane, Y. Bekakra, and A. Larabi, "Improved Backstepping Control of a DFIG based Wind Energy Conversion System using Ant Lion Optimizer Algorithm," *Period. Polytech. Electr. Eng. Comput. Sci.*, vol. 66, no. 1, pp. 43–59, 2022, https://doi.org/10.3311/PPEE.18716.
[30] B. Rached, M. Elharoussi and E. Abdelmounim, "Fuzzy Logic Control for Wind Energy Conversion System based on DFIG," *2019 International Conference on Wireless Technologies, Embedded and Intelligent Systems (WITS)*, pp. 1-6, 2019, https://doi.org/10.1109/WITS.2019.8723722.
[31] Z. Bouguerra, "Comparative study between PI, FLC, SMC and Fuzzy sliding mode controllers of DFIG wind turbine," *J. Renew. Energies*, vol. 26, no. 2, pp. 209–223, 2023, https://doi.org/10.54966/jreen.v26i2.1146.
[32] Z. Boudjema, R. Taleb, Y. Djeriri, and A. Yahdou, "A novel direct torque control using second order continuous sliding mode of a doubly fed induction generator for a wind energy conversion system," *Turkish J. Electr. Eng. Comput. Sci.*, vol. 25, no. 2, pp. 965–975, 2017, https://doi.org/10.3906/elk-1510-89.
[33] N. Bounar, S. Labdai, and A. Boulkroune, "PSO–GSA based fuzzy sliding mode controller for DFIG-based wind turbine," *ISA Trans.*, vol. 85, pp. 177–188, 2019, https://doi.org/10.1016/j.isatra.2018.10.020.
[34] W. Yin, X. Wu, and X. Rui, "Adaptive robust backstepping control of the speed regulating differential mechanism for wind turbines," *IEEE Trans. Sustain. Energy*, vol. 10, no. 3, pp. 1311–1318, 2019, https://doi.org/10.1109/TSTE.2018.2865631.
[35] A. Saci, L. Cherroun, and M. Boudiaf, "Investigation of Modeling and Control of a Grid Side System based DFIG for a Wind Turbine Machine," in *2022 19th IEEE International Multi-Conference on Systems, Signals and Devices, SSD 2022*, 2022, pp. 315–320. https://doi.org/10.1109/SSD54932.2022.9955842.
[36] F. Menzri *et al.*, "Applications of Novel Combined Controllers for Optimizing Grid-Connected Hybrid Renewable Energy Systems," *Sustain.*, vol. 16, no. 16, 2024, https://doi.org/10.3390/su16166825.
[37] N. A. N. Aldin, W. S. E. Abdellatif, Z. M. S. Elbarbary, A. I. Omar and M. M. Mahmoud, "Robust Speed Controller for PMSG Wind System Based on Harris Hawks Optimization via Wind Speed Estimation: A Real Case Study," in *IEEE Access*, vol. 11, pp. 5929-5943, 2023, https://doi.org/10.1109/ACCESS.2023.3234996.
[38] Y. Zhou, L. Zhao, and W. J. Lee, "Robustness Analysis of Dynamic Equivalent Model of DFIG Wind Farm for Stability Study," *IEEE Trans. Ind. Appl.*, vol. 54, no. 6, pp. 5682–5690, 2018, https://doi.org/10.1109/TIA.2018.2858738.
[39] H. Alnami, S. A. E. M. Ardjoun, and M. M. Mahmoud, "Design, implementation, and experimental validation of a new low-cost sensorless wind turbine emulator: Applications for small-scale turbines," *Wind Eng.*, vol. 48, no. 4, pp. 565–579, 2024, https://doi.org/10.1177/0309524X231225776.
[40] B. S. Atia *et al.*, "Applications of Kepler Algorithm-Based Controller for DC Chopper: Towards Stabilizing Wind Driven PMSGs under Nonstandard Voltages," *Sustain.* , vol. 16, no. 7, 2024, https://doi.org/10.3390/su16072952.
[41] M. Metwally Mahmoud, "Improved current control loops in wind side converter with the support of wild horse optimizer for enhancing the dynamic performance of PMSG-based wind generation system," *Int. J. Model. Simul.*, vol. 43, no. 6, pp. 952–966, 2023, https://doi.org/10.1080/02286203.2022.2139128.
[42] M. El-Shimy, "Modeling and analysis of reactive power in grid-connected onshore and offshore DFIG-based wind farms," *Wind Energy*, vol. 17, no. 2, pp. 279–295, 2014, https://doi.org/10.1002/we.1575.
[43] R. Gianto, "Steady-state model of DFIG-based wind power plant for load flow analysis," *IET Renew. Power Gener.*, vol. 15, no. 8, pp. 1724–1735, 2021, https://doi.org/10.1049/rpg2.12141.
[44] H. Boudjemai *et al.*, "Application of a Novel Synergetic Control for Optimal Power Extraction of a Small-Scale Wind Generation System with Variable Loads and Wind Speeds," *Symmetry (Basel).*, vol. 15, no. 2, 2023, https://doi.org/10.3390/sym15020369.
[45] M. M. Mahmoud, B. S. Atia, A. Y. Abdelaziz, and N. A. N. Aldin, "Dynamic Performance Assessment of PMSG and DFIG-Based WECS with the Support of Manta Ray Foraging Optimizer Considering MPPT, Pitch Control, and FRT Capability Issues," *Processe*, vol. 12, no. 10, p. 2723, 2022, https://doi.org/10.3390/pr10122723.
[46] D. Cherifi and Y. Miloud, "Evaluating Robust Constant Switching Frequency Direct Torque Control for Doubly Fed Induction Motor," *WSEAS Trans. Power Syst.*, vol. 20, pp. 297–308, 2025, https://doi.org/10.37394/232016.2025.20.23.
[47] S. Cailhol, P. E. Vidal, and F. Rotella, "A Generic Method of Pulsewidth Modulation Applied to Three-Phase Three-Level T-Type NPC Inverter," *IEEE Trans. Ind. Appl.*, vol. 54, no. 5, pp. 4515–4522, 2018, https://doi.org/10.1109/TIA.2018.2829468.
[48] H. Boudjemai *et al*., "Experimental Analysis of a New Low Power Wind Turbine Emulator Using a DC Machine and Advanced Method for Maximum Wind Power Capture," in *IEEE Access*, vol. 11, pp. 92225-92241, 2023, https://doi.org/10.1109/ACCESS.2023.3308040.
[49] M. M. Mahmoud *et al.*, "Evaluation and Comparison of Different Methods for Improving Fault Ride-Through Capability in Grid-Tied Permanent Magnet Synchronous Wind Generators," *Int. Trans. Electr. Energy Syst.*, vol. 2023, no. 1, p. 7717070, 2023, https://doi.org/10.1155/2023/7717070.
[50] M. M. Mahmoud *et al.*, "Integration of Wind Systems with SVC and STATCOM during Various Events to Achieve FRT Capability and Voltage Stability: Towards the Reliability of Modern Power Systems," *Int. J. Energy Res.*, vol. 2023, pp. 1–28, 2023, https://doi.org/10.1155/2023/8738460.
[51] M. Bouderbala, B. Bossoufi, A. Lagrioui, M. Taoussi, H. A. Aroussi, and Y. Ihedrane, "Direct and indirect vector control of a doubly fed induction generator based in a wind energy conversion system," *Int. J. Electr. Comput. Eng.*, vol. 9, no. 3, pp. 1531–1540, 2019, https://doi.org/10.11591/ijece.v9i3.pp1531-1540.

[52] M. M. Mahmoud, M. M. Aly, H. S. Salama, and A. M. M. Abdel-Rahim, "A combination of an OTC based MPPT and fuzzy logic current control for a wind-driven PMSG under variability of wind speed," *Energy Syst.*, vol. 13, no. 4, pp. 1075–1098, 2022, https://doi.org/10.1007/s12667-021-00468-2.
[53] W. Abukweik and M. Emin Tacer, "Grid Voltage-Oriented Vector Control for the Grid Side Converter of the Wind Turbine Doubly-Fed Induction Generator," *Int. J. Sci. Res.*, vol. 10, no. 4, pp. 804–810, 2021, https://doi.org/10.21275/sr21415171254.
[54] M. Elmahfoud, B. Bossoufi, M. Taoussi, N. E. Ouanjli and A. Derouich, "Rotor Field Oriented Control of Doubly Fed Induction Motor," *2019 5th International Conference on Optimization and Applications (ICOA)*, pp. 1-6, 2019, https://doi.org/10.1109/ICOA.2019.8727708.
[55] M. M. Mahmoud, M. K. Ratib, M. M. Aly, and A. M. M. Abdel–Rahim, "Application of Whale Optimization Technique for Evaluating the Performance of Wind-Driven PMSG Under Harsh Operating Events," *Process Integr. Optim. Sustain.*, vol. 6, no. 2, pp. 447–470, 2022, https://doi.org/10.1007/s41660-022-00224-8.
[56] A. A. Kadum, "PWM control techniques for three phase three level inverter drives," *Telkomnika (Telecommunication Comput. Electron. Control.*, vol. 18, no. 1, pp. 519–529, 2020, https://doi.org/10.12928/TELKOMNIKA.V18I1.12440.
[57] E. Nandhini and A. Sivaprakasam, "A Review of Various Control Strategies Based on Space Vector Pulse Width Modulation for the Voltage Source Inverter," *IETE Journal of Research*, vol. 68, no. 5. pp. 3187–3201, 2022, https://doi.org/10.1080/03772063.2020.1754935.
[58] N. Rezaei, M. N. Uddin, I. K. Amin, M. L. Othman, and M. Marsadek, "Genetic Algorithm-Based Optimization of Overcurrent Relay Coordination for Improved Protection of DFIG Operated Wind Farms," in *IEEE Transactions on Industry Applications*, pp. 5727–5736, 2019, https://doi.org/10.1109/TIA.2019.2939244.
[59] S. Heroual, B. Belabbas, T. Allaoui, and M. Denai, "Performance enhancement of a hybrid energy storage systems using meta-heuristic optimization algorithms: Genetic algorithms, ant colony optimization, and grey wolf optimization," *J. Energy Storage*, vol. 103, 2024, https://doi.org/10.1016/j.est.2024.114451.
[60] A. Guediri, M. Hettiri, and A. Guediri, "Modeling of a Wind Power System Using the Genetic Algorithm Based on a Doubly Fed Induction Generator for the Supply of Power to the Electrical Grid," *Processes*, vol. 11, no. 3, 2023, https://doi.org/10.3390/pr11030952.
[61] S. Katoch, S. S. Chauhan, and V. Kumar, "A review on genetic algorithm: past, present, and future," *Multimed. Tools Appl.*, vol. 80, no. 5, pp. 8091–8126, 2021, https://doi.org/10.1007/s11042-020-10139-6.
[62] J. Gu, "Intelligent Optimization of PID Controller Parameters Using Enhanced Parallel Genetic Algorithm," *Sci. Technol. Eng. Chem. Environ. Prot.*, vol. 1, no. 4, 2025, https://doi.org/10.61173/vday1654.
[63] J. Zhan, X. Zhu, and Y. Zhou, "Research on PID Parameter Optimisation for BP Neural Network Based on Improved Quantum Genetic Algorithm," *IET Quantum Commun.*, vol. 6, no. 1, 2025, https://doi.org/10.1049/qtc2.70024.